KINEMATIC SIMULATION AND ACCURACY TEST OF DRIVING MECHANISM OF MULTI-LINK HIGH-SPEED PRESS

Xiao MAOHUA[1*], Zhou SHUANG[2], Lu XINJIAN[3], Zhang HENGTONG[4], Wang KAIXIN[5]

In this paper, a multi-link driving mechanism is designed for a 600 KN high-speed press. Based on the assur-group method and MATLAB kinematic calculation, it is proved to have superiorities in terms of punching speed, stamping time, nominal force and mechanical advantage. ADAMS is used for kinematic simulation and the simulation results fit well with the calculated results. Its good balancing motion performance is demonstrated by the kinematic calculation of the reverse slider. The press prototype's great bottom-dead-point dynamic accuracy is tested and verified, which can provide a reference for practical manufacturing.

Keywords: Multi-link high-speed press; Kinematic analysis; MATLAB; ADAMS; Dynamic accuracy

1. Introduction

High-speed precision presses are indispensable equipment in the precision blanking process. They can produce small precision parts closer to the final shape and are important industrial equipment. High-speed precision presses can automatically feed raw materials or semi-finished products into the mold without manual labor, having the characteristics of automation, high-efficiency and high-precision [1]. High-speed precision presses have developed rapidly in

[1] Associate Prof., College of Engineering, Nanjing Agricultural University, Nanjing 210031, China, e-mail: xiaomaohua@njau.edu.cn
[2] Master, College of Engineering, Nanjing Agricultural University, Nanjing 210031, China, e-mail: 2797209524@qq.com
[3] Associate Prof., School of Mechanical Engineering, Nanjing Institute of Technology, Nanjing 211167, China, e-mail: 50547481@qq.com
[4] Master, College of Engineering, Nanjing Agricultural University, Nanjing 210031, China, e-mail: 1329901307@qq.com
[5] Master, College of Engineering, Nanjing Agricultural University, Nanjing 210031, China, e-mail: wkx592ing@126.com

developed countries in Europe, such as Germany's SMG-Feintool and Britain's Fine-O-Matic [2]. In recent years, the market's increasing demand for precision-punched parts has been driven by the rapid development of the electronics and computers industries, etc. Meanwhile, more attention is paid to the high-quality and high-efficiency of the precision parts production [3-5].

The working state of the driving mechanism directly determines the working performance of the press [6-7]. The traditional presses usually adopt the crank-slider mechanism [8]. However, its punching speed is so high that it is difficult to ensure and improve the precision of the stamping parts. Therefore, reducing the slider's punching speed becomes more important. The methods for realizing the reduction of the slider speed under the drive of a conventional motor are various, mainly including multi-link transmission, non-circular gear transmission and the like. Gao Xueqiang [9] and Li Minghao [10] did in-depth research on non-circular gear transmission, showing that its design and manufacture are difficult and not conducive to its widespread application. Compared with it, the multi-link driving mechanism has the advantages of simple structure, low manufacturing cost and reliable operation [11].

With the development of technology, many studies show that the accuracy of stamping parts and the molds' service life are also determined by the precision of presses [12]. Therefore, carrying out dynamic accuracy tests on the press is necessary. Ouyang Zhihong [13] tested the dynamic accuracy of the J23-6.3 open tilting press, considering that the vertical dynamic stiffness has a significant influence on dynamic accuracy. Zheng Anjun [14] designed a simple but effective accuracy measuring system, and verified its high reliability on the JB-04 press. Li Lechao [15] built a bottom-dead-point accuracy test platform based on LabVIEW software environment, and carried out a no-load test on a press, showing that the bottom-dead-point accuracy is deteriorated as the punching speed increases. Li Fuxing et al. [16] proposed and optimized an ideal torque calculation model for a multi-link inertial force balancing mechanism, and verified the working stability of the mechanism by using two schemes to test its bottom-dead-center precision.

As can be seen from the above analysis, a multi-link high-speed press with great dynamic accuracy can meet the needs of today's precision parts production. In this paper，a multi-link driving mechanism is designed for a 600 KN high-speed press. The main structure and working principle of it are introduced. The superior properties of the multi-link mechanism are proved by kinematic analysis. The ADAMS kinematic simulation is conducted to compare the fitting degree with the

calculated results. Then, the balancing motion analysis of the mechanism is carried out, and the test programs are designed to test the no-load high dynamic accuracy of the press prototype.

2. Multi-link Driving Mechanism of the High-speed Press

The multi-link driving mechanism is the core component of the JL75G-60 high-speed precision press. It consists of a crank-slider mechanism, a diamond-shaped mechanism and a symmetrical toggle rod mechanism in series, as shown in Fig.1. The crank-slider mechanism includes a crank 2, a connecting rod 3 and a small slider 4; the diamond-shaped mechanism includes a swinging rod 5, a swinging rod 5', a supporting rod 6 and a supporting rod 6'; the left toggle rod mechanism includes a connecting rod 7, a toggle rod 8, a ball-joint link 9, a slider 10, a secondary link 11 and a secondary slider 12, and the right toggle mechanism are symmetrical thereto.

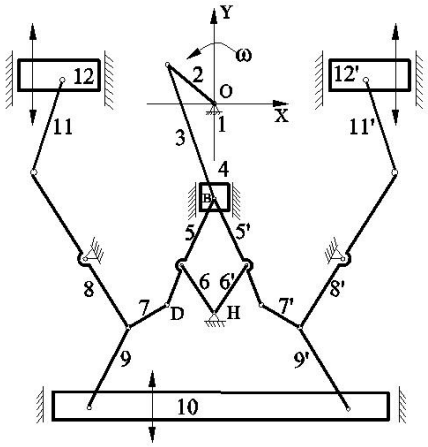

Fig. 1. Schematic diagram of the multi-link driving mechanism

The working principle of the multi-link driving mechanism is as follows. Driven by the servo motor, the rotational motion of the crank 2 is converted into the up and down reciprocating motion of the slider 4. With the up and down movement of the point B of the diamond mechanism, the position of point H can be adjusted, resulting in the movement of point D horizontally to the right and left, thereby controlling the decrease or increase of the stroke of the slider 10 to complete the stamping work. By setting a suitable speed reduction mechanism at point H, the servo motor can be used to achieve precise control of the bottom dead point. The inertial forces of the symmetrical toggle rod mechanism in the horizontal direction cancel each other out. At the same time, the secondary link

and the secondary slider are connected to the other end of the toggle rod to balance the inertial force of the reciprocating motion of the mechanism.

3. Kinematic Analysis of the Multi-link Driving Mechanism

The mechanism is symmetrical, so only the left half of it is used for kinematic analysis. Simply, the mechanism is decomposed into a link and several II-level rod groups in Fig. 2 (the upper balancing slider and the rod are not considered temporarily).

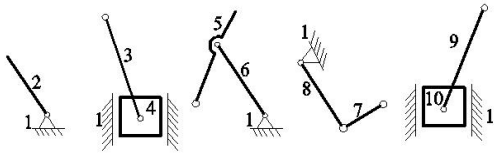

Fig. 2. Link and II-level rod groups

Taking the slider 10 as an example, as shown in Fig.3, the following kinematics equations are established.

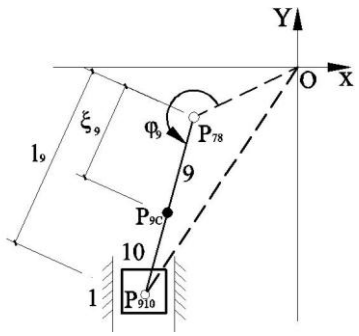

Fig. 3. Kinematic sketch of the slider 10

The displacement, velocity and acceleration of the centroid P_{9C} of the connecting rod 9 are listed as follows:

$$\left.\begin{aligned} x_{9C} &= x_{78} + \xi_9 \cos\varphi_9 \\ y_{9C} &= y_{78} + \xi_9 \sin\varphi_9 \end{aligned}\right\} \tag{1}$$

$$\left.\begin{aligned} \dot{x}_{9C} &= \dot{x}_{78} - \xi_9 \sin\varphi_9 \cdot \dot{\varphi}_9 \\ \dot{y}_{9C} &= \dot{y}_{78} + \xi_9 \cos\varphi_9 \cdot \dot{\varphi}_9 \end{aligned}\right\} \tag{2}$$

$$\left.\begin{aligned} \ddot{x}_{9C} &= \ddot{x}_{78} - \xi_9\left(\sin\varphi_9 \cdot \ddot{\varphi}_9 + \cos\varphi_9 \cdot \dot{\varphi}_9^2\right) \\ \ddot{y}_{9C} &= \ddot{y}_{78} + \xi_9\left(\cos\varphi_9 \cdot \ddot{\varphi}_9 - \sin\varphi_9 \cdot \dot{\varphi}_9^2\right) \end{aligned}\right\} \tag{3}$$

The displacement, velocity and acceleration of slider 10 are respectively:

$$s = y_{910} = y_{78} + l_9 \sin\varphi_9 \tag{4}$$

$$v = \dot{y}_{910} = \dot{y}_{78} + l_9 \cos\varphi_9 \cdot \dot{\varphi}_9 \tag{5}$$

$$a = \ddot{y}_{910} = \ddot{y}_{78} + l_9\left(\cos\varphi_9 \cdot \ddot{\varphi}_9 - \sin\varphi_9 \cdot \dot{\varphi}_9^2\right) \tag{6}$$

Based on the kinematics equations above and the parameters listed in *Table 1*, the displacement, velocity and acceleration curves of the slider 10 are plotted in the MATLAB environment, in which the crank speed is set to 600rpm. For comparison, the motion curves of the crank-slider mechanism are also given (the stroke is 25 mm, and the connecting rod coefficient is 0.04).

Table 1

Mass, centroid position and moment of inertia of each rod and slider

Components	Mass (kg)	Centroid position ξ_i (mm)	Moment of inertia J_{ic} ($\times 10^5$kg.mm^2)
Crank 2	127	5.8	2.96
Connecting rod 3	181	122.2	58.3
Slider 4	62.5	-	-
Swinging rod 5	30.5	140.9	6.27
Supporting rod 6	25.5	69.7	2.12
Connecting rod 7	15.9	90.5	1.55
Toggle rod 8	142.6	104.2	32.2
Link 9	37.1	89.2	5.27
Slider 10	1100	-	-

Figure 4 is the displacement curves of sliders. The slider displacement curve of the multi-link mechanism is below, and the change is relatively gentle near the bottom dead point. Besides, the crank angle is 134° when it reaches the nominal force stroke, while the crank angle of the crank-slider mechanism is 155°, so the punching time can be extended by 80%. It is beneficial to reduce the vibration and noise generated during the blanking process [17].

Figure 5 is the velocity curves of sliders. The absolute value of the slider velocity of the multi-link mechanism between 87° and 275° is significantly smaller (except for the bottom dead point position). In the nominal force stroke, the speeds of the multi-link and crank-slider mechanisms are -281.5mm/s and -437.1mm/s, respectively, and the former is only 64.6% of the latter. According to the definition of the slider speed simulation, the multi-link mechanism under the

same torque can produce an extra 55.3% nominal force, and it has a significant labor-saving effect.

Figure 6 is the acceleration curves of sliders. The multi-link mechanism produces a very large acceleration of -97.6m/s^2 at 0° and 360°, and the crank-slider mechanism is -41.9 m/s^2. The former is 2.3 times the latter, indicating that the multi-link press needs larger starting torque. However, at the bottom dead point, the slider acceleration of the multi-link mechanism is only 30.7% of the other. In the nominal force stroke, the acceleration of the multi-link mechanism and crank-slider mechanism are 30.1 m/s^2 and 48.9 m/s^2, the former being only 61.6% of the latter. During the working process, the inertial force generated will cause the bottom dead point to shift downward. Smaller acceleration is beneficial to reduce it and improve the dynamic accuracy of the bottom dead point.

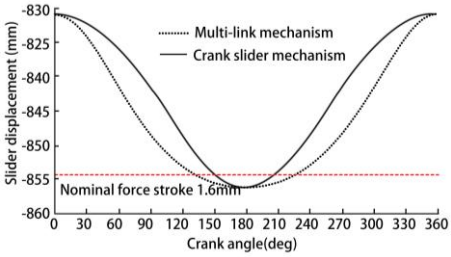

Fig. 4. Displacement curves of sliders

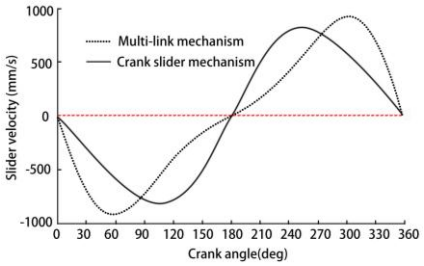

Fig. 5. Velocity curves of sliders

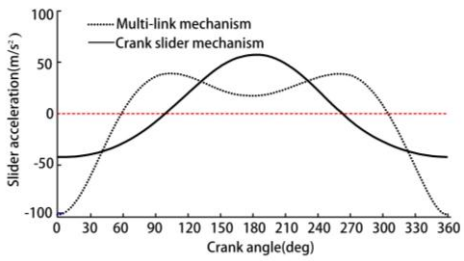

Fig. 6. Acceleration curves of sliders

The calculation formula for mechanical advantage is:

$$\frac{FH}{M}=\frac{H}{dh/d\theta}=\frac{H}{\upsilon/\omega} \tag{7}$$

where F is the punching force (KN); H is the slider stroke (mm); M is the driving torque (N.m); dh is the slider micro-displacement (mm); $d\theta$ is the micro-turn of the crank (rad); υ is the slider velocity (mm/s); ω is the crank angular velocity (rad/s).

In the nominal force stroke, the mechanical advantages of the multi-link mechanism and the crank-slider mechanism are 5.58 and 3.59, respectively, and the former is 1.55 times the latter. Therefore, the multi-link mechanism has better mechanical advantage.

4. ADAMS Simulation Results and Balancing Motion Analysis

The kinematic simulation of slider 10 in ADAMS are as shown in Fig. 7. It can be seen that the corresponding angle is about 134° when the nominal force stroke is reached. When the crank angle is 58° and 300°, the slider speed reaches the maximum of -922.6mm/s and 922.6mm/s. The slider speed at the nominal force stroke is -281.5mm/s. The slider acceleration reaches -97.6m/s^2 at the top dead point and reaches 17.4m/s^2 at the bottom dead point. The acceleration at the nominal force stroke is 30.1m/s^2. The kinematic simulation results are greatly consistent with the theoretical values calculated in the previous chapter.

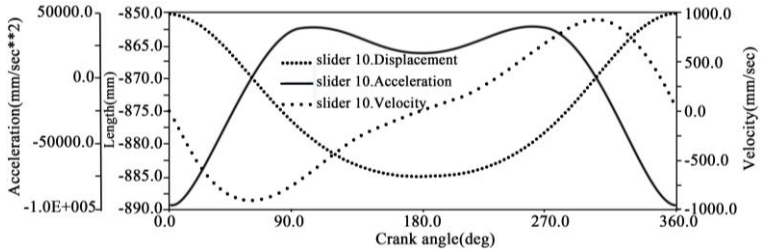

Fig. 7. The displacement, velocity and acceleration curves of the slider 10

Besides, the link 11, the slider 12, and the toggle rod 8 of the driving mechanism are taken into consideration to perform balancing motion analysis. The mass, centroid position and moment of inertia are shown in *Table 2*.

Table 2

Mass, centroid position, moment of inertia of components

Components	Mass(kg)	Centroid position ξ_i(mm)	Moment of inertia J_{iC}(×10^{5}kg.mm^2)
Link 11	25.5	137	5.9
Slider 12	583	-	-
Toggle rod 8	191.4	24	71.8

Figure 8 is an acceleration curve of slider 12, which is exactly the opposite of the acceleration curve of slider 10. Specifically, at the top and bottom dead point positions, the acceleration of slider 12 is 97.6 m/s^2 and -17.4 m/s^2, respectively, which are opposite to the acceleration of slider 10. They have great balancing motion performance.

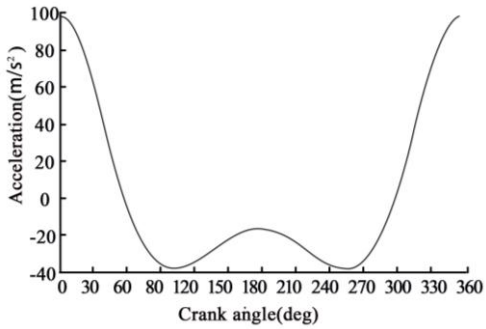

Fig. 8. Acceleration curve of the slider 12

Particularly, six crank angles are randomly selected to obtain the acceleration of the slider 10 and the slider 12, as shown in *Table 3*. The data shows that the two sliders still satisfy the law that the acceleration values are equal and the directions are opposite.

Table 3

Accelerations of slider 10 and slider 12 with the same crank angle

Crank angle (deg)	Acceleration of slider 10 (m/s$^{2)}$	Acceleration of slider 12 (m/s$^{2)}$
35	-50.6	50.6
45	-28.1	28.1
100	38.6	-38.6
196	19.0	-19.0
293	16.7	-16.7
328	-52.9	52.9

5. Dynamic Accuracy Test and Verification

The press prototype is manufactured, consisting of the body (upper beam, lower beam, column and 4 tie rods), crankshaft clutch, multi-link driving mechanism and slider, as shown in Fig. 9 (a).

To verify the accuracy of the multi-link high-speed press, the dynamic accuracy test is carried out. The measuring device is shown in Fig. 9(b). Using the two-channel measurement method, the positions of the two guide posts in front of the slider are measured, and the two values are CH_1 and CH_2, respectively. The slider parallelism at the bottom dead point ($P_{b.d.p}$) can be expressed as:

$$P_{b.d.p} = CH_1 - CH_2 \tag{8}$$

(a) press prototype (b) test device

Fig. 9. Experimental machine tool and equipment

Test programs are as follows.

Rising Temperature and Constant Speed. Run at a constant speed for 3 hours from the initial state. Working speeds are 200spm, 250spm and 300spm, respectively. When changing the speed, the downtime should be more than 10h.

Constant Temperature and Speed. After the previous step is completed, if the bottom dead point no longer continuously offset, the machine tool will reach a thermal equilibrium state. The next continuous measurement is more than 0.5h.

The data in Fig.10 is measured by the "Rising Temperature and Constant Speed" program, which reflects the $P_{b.d.p}$ changes at constant speeds. As Fig. 10(a) shows, when the test was carried out for 102 minutes, the data of CH_1 overflowed and the $P_{b.d.p}$ accumulated a deviation of 35μm. After stopping the machine for a few minutes and re-sampling, the $P_{b.d.p}$ quickly reduced to an average of 1.2μm. In Fig. 10(b), the amplitude of parallelism change is less than 30μm within 3 hours, and the average is 3μm. In Fig. 10(c), the inverter current increases abnormally at 47 minutes and the $P_{b.d.p}$ reaches a maximum of -58μm. After re-sampling, the $P_{b.d.p}$ becomes smaller and its average is measured as -7.74μm. The above data results show that the $P_{b.d.p}$ is within 35μm under normal circumstances, which are small enough to meet the expected accuracy requirements.

The three groups of experiments shown in Fig.11 are conducted to verify the stability of the press at constant temperature and speed. In Fig.11(a) and Fig.11(b), the deviation ranges are within 11μm and 19μm, respectively. As time goes on, the parallelism deviation fluctuates around the zero point. Figure11(c) is a $P_{b.d.p}$ curve obtained by continuous testing within 30 minutes at a speed of 300spm. The maximum, minimum and average value of $P_{b.d.p}$ are 7μm, -27μm and -5.43μm, respectively. In addition, the standard deviations of the three experiments are 2.54μm, 4.15μm and 8.79μm, respectively, indicating that the dispersion degree of the $P_{b.d.p}$ is low. So it is easy to find that the press keeps good bottom-dead-point accuracy and stability under long-term operating conditions.

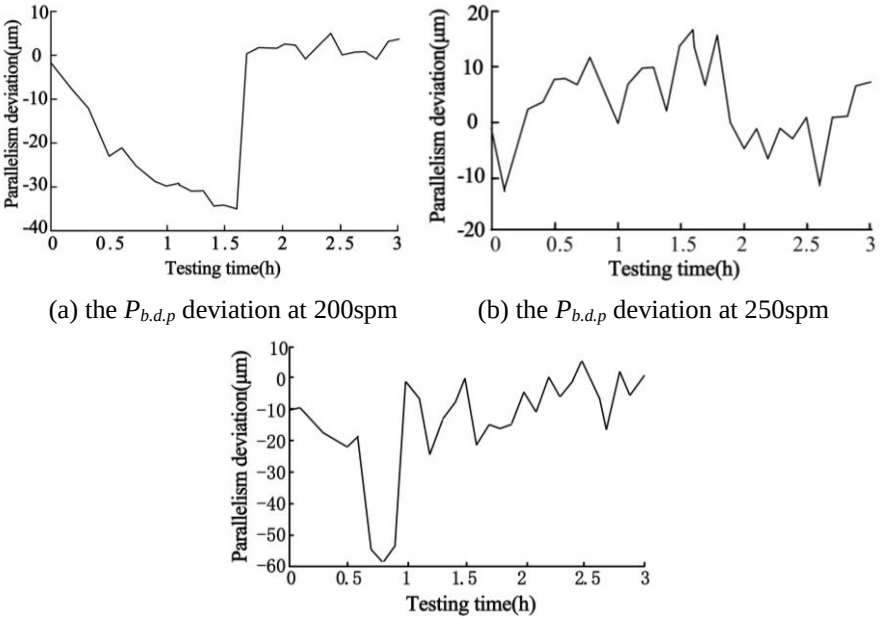

(a) the $P_{b.d.p}$ deviation at 200spm (b) the $P_{b.d.p}$ deviation at 250spm

(c) the $P_{b.d.p}$ deviation at 300spm

Fig. 10. The $P_{b.d.p}$ deviations of slider 10 within 3 hours at different speeds

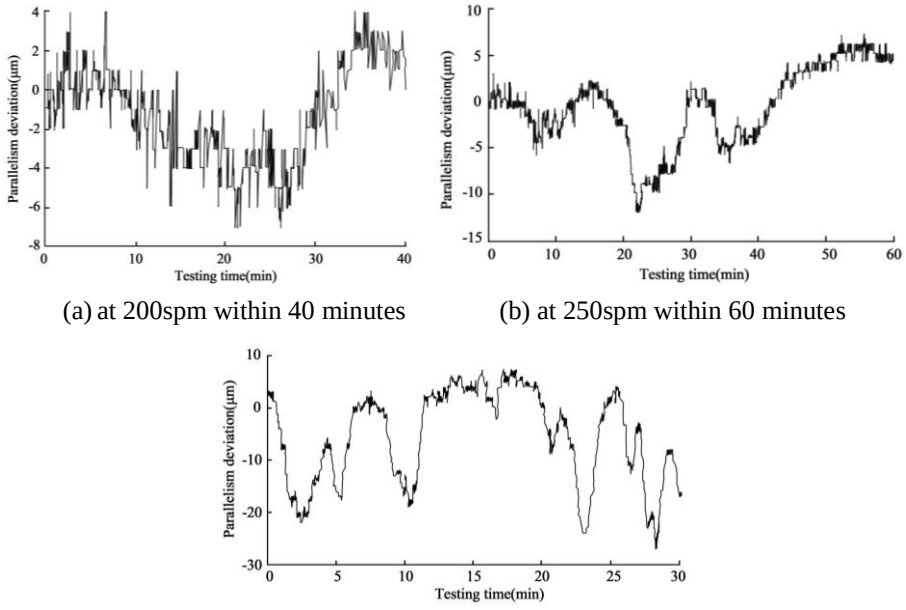

(a) at 200spm within 40 minutes (b) at 250spm within 60 minutes

(c) at 300spm within 30 minutes

Fig. 11. The $P_{b.d.p}$ deviations of slider 10 at constant temperatures and speeds

After analyzing the experiment results above, it can be concluded that the slider parallelism at the bottom dead point has high accuracy and operational

stability, so it can be a good example for practical manufacturing.

6. Conclusions

In this paper, a multi-link driving mechanism is proposed, whose good performance is proved by several methods, including kinematic analysis, MATLAB and ADAMS simulation and dynamic accuracy test.

(1) Compared with the crank-slider mechanism, the stamping time of the multi-link mechanism is extended by 80%. With the same driving torque, the nominal force of about 55.3 % can be obtained over the crank-slider mechanism. In the nominal force stroke, its acceleration is only 61.6% of that of the crank-slider mechanism. Its mechanical advantage is 1.55 times that of the crank-slider mechanism. The multi-link press has the characteristics of low punching speed and low acceleration near the bottom dead point, which is beneficial to improve the bottom-dead-point accuracy.

(2) The upper and the lower sliders satisfy the law that the acceleration absolute values are equal and the directions are opposite. The mechanism has good balancing motion performance.

(3) The small averages and standard deviations are calculated, verifying the favorable accuracy and stability of the slider parallelism at the bottom dead point, respectively. The multi-link driving mechanism can be used as a practical press manufacturing.

In future research, a multi-link driving mechanism model with clearances will be established for ADAMS simulation to study the effects of clearances and friction coefficients on the press speed. Also, a four-channel test will be designed and conducted to study the influence of the parameters of oil temperature control system on the bottom-dead-point dynamic accuracy.

Acknowledgments

The research is supported by the Key Research and Development Program of Jiangsu Province (BE2018127).

R E F E R E N C E S

[1]. *Y. Li, L. Rong, L. Z. Tian, et al.*, “Application of high-speed press in new industries”, in China Metalforming Equipment & Manufacturing Technology, **vol. 54**, no. 3, Jun. 2019, pp.42-44.

[2]. *M. Deng, G. M. Hu, L. Lin, et al.*, “Present situation and development trend of fine blanking press”, in Forging & Stamping Technology, **vol. 41**, no. 8, Aug. 2016, pp. 1-6.

[3]. *L. Z. Xiang, C. Q. Wang*, “Control system design of fine-blanking machines based on PLC”, in

China Measurement & Test, **vol. 39**, no. 2, Mar. 2013, pp. 98-101.

[4]. *S. D. Zhao, X. L. Zhang, C. Y. Gao, et al.*, "Actuality & progress of high speed press", in China Metalforming Equipment & Manufacturing Technology, **vol. 40**, no. 1, Feb.2005, pp.17-25.

[5]. *Q. X. Xia, X. T. Hu, D. Chen, et al.*, "Current research and development tendency of fine blanking technology", in Forging & Stamping Technology, **vol. 40**, no. 7, Jul. 2015, pp. 1-6.

[6]. *Z. M. Ke, X. J. Lu, H. W. Feng, et al*, "Research on new drive mechanism of a high-speed precision press", in China Forging Equipment & Manufacturing Technology, **vol. 48**, no. 3, Mar. 2013, pp. 33-34.

[7]. *W. Ding, W. X. Ding, B. B. Feng*, "Dynamic simulation for press transmission system based on ADAMS", in Manufacturing Automation, **vol. 32**, no. 12, Nov. 2010, pp. 87-89.

[8]. *C. K. He*, "Kinematic characteristics analysis of multi-link high-speed press", in China Metalforming Equipment & Manufacturing Technology, **vol. 48**, no. 5, Oct.2013, pp.19-21.

[9]. *X. Q. Gao, S. Q. Yang, L.Ma*, "Optimum scheme for connecting noncircular gears and crank-slider mechaniam", in Journal of Taiyuan University of Technology, **vol. 33**, no. 1, Jan. 2002, pp. 41-43.

[10]. *M. Y. Li, Y. H. Gong, Z. H. Zhao*, "Kinematic characteristic of press with ellipse gear transmitting", in Forging & Stamping Technology, no. 6, Dec. 2006, pp. 87-90.

[11]. *Y. P. He, C. H. Zou, Z. H. Yuan, et al.*, "Optimization design of multi-bar mechanical press based on genetic algorithm", in Journal of Henan Agricultural University, **vol. 39**, no. 4, Dec. 2005, pp. 95-97.

[12]. *C. L. Liu*, "Influence of press precision on stamping parts", in Forging & Stamping Technology, no. 5, Oct. 1999, pp. 32-33+53.

[13]. *Z. H. OuYang, X. P. Jie*, "The dynamic accuracy and frame rigidity of the gap mechanical press", in Journal of Jiangxi Polytechnic University, **vol. 11**, no. 1, Jan. 1989, pp. 98-105.

[14]. *A. J. Zheng, L. M. Yao, X. S. Wang*, "Measuring of bottom center precision in mechanical press", in China Metalforming Equipment & Manufacturing Technology, no. 6, Dec. 2007, pp. 22-24.

[15]. *L. C. Li*, "Research and development of key dynamic characteristic parameter test system for press", in Nanjing University of Science and Technology, 2008.

[16]. *F. X. Li, H. Liu, M. L. Li, et al.*, "Driving torque model and accuracy test of multilink high-speed punch", in Mathematical Problems in Engineering, **vol. 2018**, no. 5, May. 2018, pp. 1-10.

[17]. *B. M. Jiang, X. Y. Zhou, Y. X. Zhou, et al.*, "Vibration analysis and control of high-speed press", in China Metalforming Equipment & Manufacturing Technology, **vol. 52**, no. 2, Apr. 2017, pp. 28-31.